molecular pharmaceutics

Article

pubs.acs.org/molecularpharmaceutics

Thermodynamic Phase Behavior of API/Polymer Solid Dispersions

Anke Prudic, Yuanhui Ji, and Gabriele Sadowski*

Department of Biochemical and Chemical Engineering, Laboratory of Thermodynamics, TU Dortmund, Emil-Figge-Str. 70, D-44227 Dortmund, Germany

Supporting Information

ABSTRACT: To improve the bioavailability of poorly soluble active pharmaceutical ingredients (APIs), these materials are often integrated into a polymer matrix that acts as a carrier. The resulting mixture is called a solid dispersion. In this work, the phase behaviors of solid dispersions were investigated as a function of the API as well as of the type and molecular weight of the carrier polymer. Specifically, the solubility of artemisinin and indomethacin was measured in different poly(ethylene glycol)s (PEG 400, PEG 6000, and PEG 35000). The measured solubility data and the solubility of sulfonamides in poly(vinylpyrrolidone) (PVP) K10 and PEG 35000 were modeled using the perturbed-chain statistical associating fluid theory (PC-SAFT). The results show that PC-SAFT predictions are in a good accordance with the experimental data, and PC-SAFT can be used to predict the whole phase diagram of an API/polymer solid dispersion as a function of the kind of API and polymer and of the polymer's molecular weight. This remarkably simplifies the screening process for suitable API/polymer combinations.

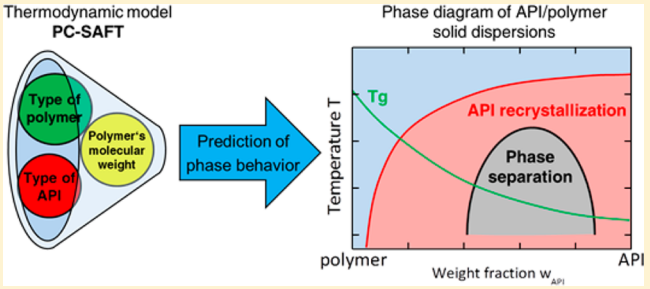

KEYWORDS: *poorly soluble pharmaceutical, phase behavior, molecular weight of polymer, indomethacin, artemisinin, thermodynamic model, PC-SAFT*

INTRODUCTION

Many promising active pharmaceutical ingredients (APIs) are limited in bioavailability due to their low solubility and/or slow dissolution rate in aqueous media. A promising strategy to enhance the dissolution behavior is the integration of APIs into a carrier matrix (e.g., a polymer) to formulate a so-called solid dispersion.[1−3] The solubility of the crystalline API in and the miscibility of the amorphous API with the polymer define the maximum API loading in a polymer without recrystallization or phase separation.[4] Therefore, knowledge about the thermodynamic phase behavior is essential for the design of long-term stable solid dispersions, especially in the case of amorphous solid dispersions.

In addition to storage conditions such as temperature and relative humidity, the phase behavior of API/polymer solid dispersions depends on the API, the polymer used as carrier matrix, and also the molecular weight of the polymer.[5−8] These properties have to be considered when discussing the solubility and the dissolution rate for appropriate API/polymer combinations.[9] Although it is quite obvious that the knowledge of the thermodynamic phase behavior is very important, experimental results for these systems are rather limited in the literature.

The solubility of crystalline APIs is usually determined by the dissolution-end point method using differential scanning calorimetry (DSC).[10,11] This method, however, has limitations because the resulting endothermic signals are sometimes too small for evaluation, depending on the polymer type and the API/polymer composition. To ensure thermodynamic equilibrium, different heating rates are chosen, and the melting temperature of the API/polymer mixture is obtained by extrapolating to heating rate zero.[12]

The experimental investigation of the liquid−liquid phase separation of fully amorphous solid dispersions is even more difficult. Because of the high viscosity of the polymer systems, phase separation occurs very slowly and can take many weeks or even years.[4] Since experimental investigation of the phase behavior of API/polymer solid dispersions is time-consuming and challenging, the application of a thermodynamic model that is able to describe or predict the whole phase diagram including the solubility line of the crystalline API and liquid−liquid phase separation is very worthwhile to reduce the experimental effort.

There are several reports available that model the crystalline API solubility in polymers or the liquid−liquid phase separation of API/polymer solid dispersions using either the Flory−Huggins theory[13] or Hansen's solubility parameters[14] or a combination of both.[11,15,16] The Flory−Huggins theory, however, cannot consider specific molecular interactions, e.g., the formation of hydrogen bonds or dipole−dipole interactions. Moreover, the Flory−Huggins binary parameter χ usually does not only depend on the kind of API and polymer but also on temperature, API/polymer composition, and the polymer molecular weight. Therefore, it can be used for correlation of

Received: December 5, 2013
Revised: April 14, 2014
Accepted: May 16, 2014
Published: May 16, 2014

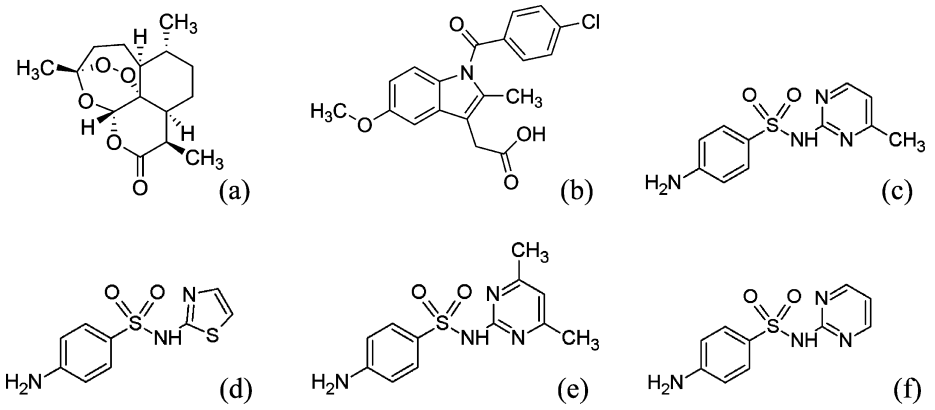

Figure 1. Chemical structures of artemisinin (a), indomethacin (b), sulfamerazine (c), sulfathiazole (d), sulfadimidine (e), and sulfadiazine (f).

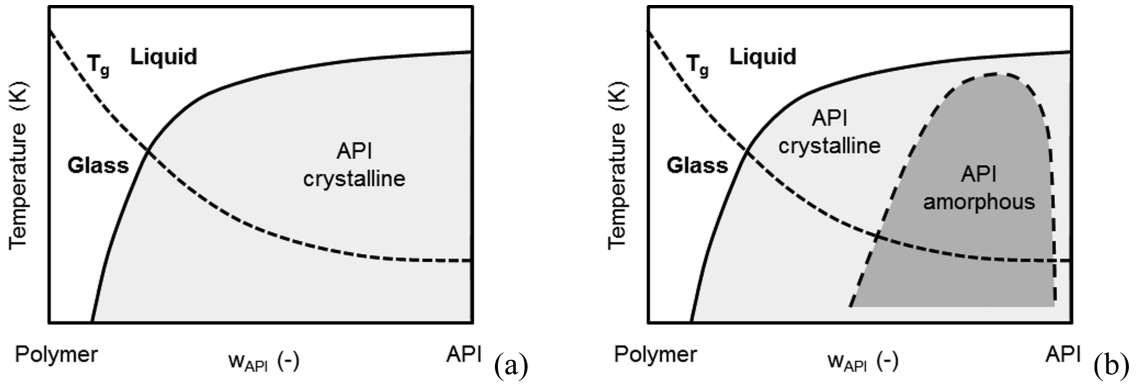

Figure 2. Schematic phase diagrams of API/polymer dispersions. The solid line represents the solubility line of the crystalline API in the polymer, the short-dashed line represents the glass-transition line of a freshly prepared (hypothetically homogeneous) API/polymer dispersion, and the dashed line surrounds the demixing region of the amorphous API/polymer dispersion (LLE). The occurrence of the latter depends on the API and the polymer: (a) system without amorphous phase separation and (b) system with amorphous phase separation.

known experimental data but extrapolations to other experimental conditions are very unsure.[17]

The same restrictions apply to the Hansen solubility parameters. On the basis of the chemical structure of a compound, one three-dimensional solubility parameter is calculated, which accounts for the interaction energy between two molecules. This parameter is obtained empirically as the sum of different contributions, such as dispersive, polar, and hydrogen-bonding interactions.[14] The use of this parameter for miscibility studies is based on the assumption that two different compounds with similar solubility parameters (similar interaction energies) have high mutual solubility. This assumption, however, neglects that the solubility of two components does not only depend on the system's enthalpy (which is accounted for by the Hansen parameters) but also on its entropy, which of course limits its applicability. Nevertheless, this approach is often used to perform a fast and qualitative screening of appropriate API/polymer combinations. A quantitative description of solubility data or an extrapolation to temperatures other than 25 °C, however, requires an additional experimental effort.

In this work, we apply a physically sound thermodynamic model to describe the phase behavior of API/polymer dispersions, the perturbed-chain statistical associating fluid theory (PC-SAFT).[18] Within PC-SAFT, each molecule (e.g., solvent, polymer, or API) is considered as a chain of spherical segments that can interact with segments of other molecules through different types of interactions. In particular, chain-like structures (in particular important for polymer systems), repulsive interactions, van der Waals attractions, the formation of hydrogen bonds, dipole−dipole interactions, and charges can be specifically considered.

Each molecule is characterized by a number of pure-component parameters that can be determined by fitting to easily assessable experimental data, e.g., vapor pressures, liquid densities, or, specifically in the case of solids, solubility data in solvents. As soon as these pure-component parameters are known for every molecule in a mixture, the thermodynamic properties of this mixture, e.g., density, enthalpy, entropy, component chemical potentials, vapor pressures, solubilities, and liquid−liquid demixing can be calculated as a function of temperature, pressure, and composition.

Although PC-SAFT expressions (see Supporting Information) are more complex and the model requires more pure-component parameters than, e.g., Flory−Huggins theory, it has the enormous advantage that all parameters have a physical meaning and do not depend on anything than just on the particular component. Moreover, PC-SAFT allows to fully predict the behavior of polymer systems as a function of polymer molecular weight and of copolymer systems based only on the knowledge of the respective homopolymers without any further parameter fitting.[19] Prediction of ternary and higher systems (as, e.g., required to model the influence of humidity on polymer/API systems) based on the knowledge of binary data only is usually quite successful.[20,21]

PC-SAFT has been widely used in literature for a huge number of systems containing gases,[22] solvent molecules,[21,23,24]

dx.doi.org/10.1021/mp400729x | Mol. Pharmaceutics 2014, 11, 2294−2304

polymers,[25,26] and solids,[27,28] and PC-SAFT parameters have already been determined for more than 400 components.[29−31] More recently, PC-SAFT was also used to calculate the solubility of crystalline APIs (solid−liquid equilibrium; SLE) in organic solvents and solvent mixtures,[28] to consider the pH dependence of the API solubility in aqueous media,[32] and to predict the "oiling-out" phenomenon during crystallization processes.[33] From a thermodynamic point of view, the latter is similar to the phase separation (liquid−liquid equilibrium; LLE) of an API/polymer solid dispersion, which is described in the next section of this work.

In this work, PC-SAFT is for the first time applied to model the solubility of APIs in polymers. Artemisinin and indomethacin as well as four different sulfonamides (sulfamerazine, sulfathiazole, sulfadimidine, and sulfadiazine) were chosen as examples for APIs. Their chemical structures are shown in Figure 1.

Poly(ethylene glycol) (PEG) was chosen as the model polymer because it is available in a liquid state at low molecular weights and in a solid state at higher molecular weights. The solubility of artemisinin and indomethacin in different PEGs (PEG 400, PEG 6000, and PEG 35000) and of sulfathiazole and sulfadimidine in PEG 35000 was investigated experimentally and modeled with PC-SAFT. Moreover, this model was used to predict the influence of the polymer molecular weight on the API/polymer phase behavior for different molecular weights of PEG.

To evaluate the predictive capability of PC-SAFT, the solubilities of four different sulfonamides (sulfamerazine, sulfathiazole, sulfadimidine, and sulfadiazine) in poly(vinylpyrrolidone) (PVP K10) and additionally of sulfathiazole and sulfadimidine in PEG 35000 were predicted, and the modeling results were compared to the experimental data.

Phase Behavior of API/Polymer Dispersions. Figure 2 shows schematic phase diagrams of API/polymer dispersions.

The solubility line in Figure 2a describes the solubility of the crystalline API in the polymer. This line is thus determined by the solid−liquid equilibrium (SLE) of the API/polymer dispersion. As long as the considered polymer is amorphous (e.g., PVP) or in the molten state (e.g., PEG at temperatures higher than 338.15 K), the polymer acts as a solvent and the crystalline API acts as a solute. The solubility line describes the amount of API that can be dissolved into a polymer carrier without (re)crystallization. This quantity depends on temperature and relative humidity, which must be considered when choosing certain storage conditions.[34]

Above the solubility line, the homogeneous liquid dispersion of the API and the polymer is thermodynamically stable, and therefore, there is no risk of (re)crystallization. Below the solubility line, the API tends to recrystallize, which might invalidate the bioavailability-improving effect of a solid dispersion. It should also be noted that crystallization does not necessarily take place at the thermodynamic solubility line and is usually kinetically hindered due to the high viscosity of the dispersion. This often leads to metastable solid dispersions, which may crystallize at much lower temperatures and/or after very long times.

In some cases, these metastable solid dispersions also exhibit a separation into two amorphous phases (LLE): an API-rich phase and a polymer-rich phase. The LLE is often called the miscibility of the amorphous API and the polymer.[35,36] In fact, an amorphous solid dispersion of an API and a polymer tends to demix at all temperatures/compositions within the LLE region and tends to recrystallize at all temperatures/compositions below the solubility line.

Thus, the location of both, the solubility line and the LLE region is most important for providing a homogeneous dosage (e.g., in a tablet). Figure 2a,b shows that the homogeneous amorphous dosage at high API concentrations can only be achieved at high temperatures (above both the solubility line and, in the case of an amorphous demixing, above the LLE region). However, the temperature of application is usually given by the human-body environment and therefore cannot be freely chosen. Thus, most amorphous solid dispersions that are used for medical applications are thermodynamically metastable and tend to recrystallize or demix into two amorphous phases.

Fortunately, the homogeneous state can be preserved to a certain extent by keeping the storage temperatures below the glass-transition temperature of the dispersion (see Figure 2a,b). In this region, the mobility of the molecules is drastically reduced, and the time for phase separation or recrystallization can take up to several months or even years.[37] The glass transition of API/polymer solid dispersions can easily be determined by DSC measurements or estimated using the Gordon−Taylor/Kelly−Bueche equation.[38,39]

Finally, it needs to be mentioned that Figure 2a,b shows the phase behavior of a water-free system. Humidity and therewith a certain water content in the solid dispersion can drastically affect the phase behavior of the solid dispersion because it can cause quantitative changes in the phase diagram and can decrease the viscosity, often reducing the time for demixing and/or recrystallization. This will be discussed in a subsequent paper.

Thermodynamic Calculation of Solubility and Miscibility. The solubility of a crystalline API in a polymer is determined by the thermodynamic equilibrium (SLE) of the crystalline API solid and the liquid API/polymer phase. The API concentration of the latter is usually called the API solubility in the polymer.

At the SLE, the chemical potential of the API in the solid phase equals that in the liquid phase. Assuming a pure solid phase, the solubility can be calculated as follows:[40]

$$x_{\mathrm{API}}^{\mathrm{L}} = \frac{1}{\gamma_{\mathrm{API}}^{\mathrm{L}}} \exp\left[-\frac{\Delta h_{\mathrm{API}}^{\mathrm{SL}}}{RT}\left(1 - \frac{T}{T_{\mathrm{API}}^{\mathrm{SL}}}\right) - \frac{\Delta c_{p,\mathrm{API}}^{\mathrm{SL}}}{R} \left(\ln\left(\frac{T_{\mathrm{API}}^{\mathrm{SL}}}{T}\right) - \frac{T_{\mathrm{API}}^{\mathrm{SL}}}{T} + 1\right)\right] \quad (1)$$

$x_{\mathrm{API}}^{\mathrm{L}}$ is the solubility of the API (mole fraction), R is the universal ideal gas constant, and T is the temperature of the system in Kelvin. $T_{\mathrm{API}}^{\mathrm{SL}}$, $\Delta h_{\mathrm{API}}^{\mathrm{SL}}$and $\Delta c_{p,\mathrm{API}}^{\mathrm{SL}}$ are the melting temperature, the heat of fusion, and the difference in the solid and the liquid heat capacities of the API, respectively. These properties can be determined experimentally (e.g., by DSC measurements). $\gamma_{\mathrm{API}}^{\mathrm{L}}$ is the activity coefficient of the API in the liquid API/polymer phase. This is the only value that depends on the polymer used because all other quantities mentioned so far are pure-component properties of the API. The activity coefficient depends on temperature and on composition of the API/polymer dispersion and is a measure for the differences in molecular shapes and molecular interactions of the API and the polymer. Only in cases where these molecules have identical shapes and molecular interactions, the activity coefficient $\gamma_{\mathrm{API}}^{\mathrm{L}}$ would be equal to one. Obviously, this is not the case for solid

dispersions because the molecules are very different. Therefore, one needs to determine the activity coefficient γ^{L}_{API} of the API as a function of the type and molecular weight of the polymer and of composition and temperature. For that purpose, PC-SAFT was used in this work.

The LLE describes the miscibility of an amorphous API and polymer. To calculate the LLE, the chemical potentials of both, the API and the polymer, have to be identical in the two liquid phases, L1 and L2, leading to the following phase-equilibrium conditions:

$$x^{L1}_{polymer}\gamma^{L1}_{polymer} = x^{L2}_{polymer}\gamma^{L2}_{polymer} \quad (2)$$

$$x^{L1}_{API}\gamma^{L1}_{API} = x^{L2}_{API}\gamma^{L2}_{API} \quad (3)$$

x_i^{L1} and x_i^{L2} represent the concentrations of the API and the polymer in the two phases, L1 and L2, and $\gamma_i^{L1}$and γ_i^{L2} are the activity coefficients of the API and the polymer in these phases.

To estimate the activity coefficients γ_i^{L1} and γ_i^{L2} of the API and the polymer, again, PC-SAFT was applied in this work.

PC-SAFT. Within PC-SAFT, the residual Helmholtz energy a^{res} of a system is considered as a sum of different Helmholtz-energy contributions (see eq 4).[18,21] PC-SAFT accounts for contributions due to repulsion of molecules, which are allowed to have different sizes (hard-chain contribution a^{hc}), van der Waals attractions (dispersion a^{disp}), and association (a^{assoc}):[21]

$$a^{res} = a^{hc} + a^{disp} + a^{assoc} \quad (4)$$

Moreover, there exist specific contributions to account for dipole−dipole interactions and charged species, which should be mentioned but are not required for modeling the molecules considered within this work.

By considering the different contributions, PC-SAFT allows explicitly to account for the physics of the molecules and the different interactions that might occur in an API/polymer dispersion. Depending on the nature of the considered molecules, only the first two contributions or also the specific interactions, such as association, dipole−dipole interactions, or even ionic interactions, can be considered within the modeling. The expressions used for calculating the different contributions are given in the Supporting Information and are also described elsewhere in more detail.[18]

As a short introduction into the basic ideas of the model, the different parameters and quantities are explained as follows. PC-SAFT treats a molecule i (API, polymer, or any other molecule) as a chain consisting of m_i^{seg} spherical segments of diameter σ_i (see Figure 3 for indomethacin as an example).

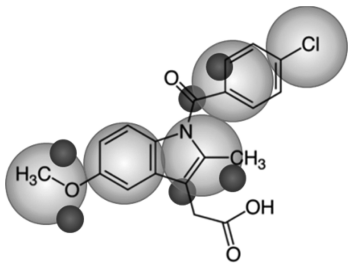

Figure 3. PC-SAFT scheme of indomethacin described as a chain consisting of spherical segments (gray) and N_i^{assoc} association sites (black). In this example, N_i^{assoc} equals six; three electron acceptors and three electron donors.

These chains interact with each other. The repulsive interactions are described by the hard-chain contribution in eq 4. This contribution depends on the number of molecular segments, m_i^{seg}, and on the segment diameter, σ_i. The Helmholtz-energy contribution a^{disp}, which accounts for the van der Waals attraction of segments from different molecules, depends on the interaction energy between two segments u_i (also called the dispersion energy). Thus, each component is characterized by at least three pure-component parameters: the segment number m_i^{seg}, the segment diameter σ_i, and dispersion-energy parameter u_i/k_B (k_B is the Boltzmann constant).

As APIs and polymers in pharmaceutical systems are often able to form hydrogen bonds, the Helmholtz contribution for association, a^{assoc}, is also included here. For that purpose, the number of possible association sites, N_i^{assoc}, is defined for each molecule based on its molecular structure. In the case of indomethacin (as shown in Figure 3), six association sites (three electron acceptors and three electron donors) were considered. Calculating the Helmholtz-energy contribution, a^{assoc}, requires two more pure-component parameters, namely, the association-energy parameter ε^{AiBi}/k_B (related to the strength of association) and the association-volume parameter κ^{AiBi} (related to the distance between two molecules necessary to form a hydrogen bond). Therefore, in total, five pure-component parameters are used to characterize a molecule that is able to interact by hydrogen bonding.

For solvents, the pure-component parameters are usually fitted to the vapor pressures and liquid densities of the pure components. For many solvents, these properties are already available in the literature.[26] Since vapor pressures and liquid densities are usually not measurable for either solid APIs or polymers, the pure-component parameters of APIs and polymers are usually determined by fitting to experimental solubility data of these components in organic solvents.[26,28] For the APIs and polymers used in this work, this is described in the Results section.

Determination of activity coefficients from PC-SAFT. The activity coefficient γ_i^L for a polymer or an API is obtained as the ratio of the fugacity coefficient φ_i^L of the respective component in the API/polymer dispersion and the fugacity coefficient φ_{0i}^L of the pure liquid compound i:

$$\gamma_i^L = \frac{\varphi_i^L}{\varphi_{0i}^L} \quad (5)$$

The fugacity coefficient φ_i^L of the polymer and the API can be calculated after determination of the residual chemical potential μ_i^{res} and the compressibility factor Z according to

$$\ln \varphi_i^L = \frac{\mu_i^{res}}{k_B T} - \ln Z \quad (6)$$

Both, the compressibility factor Z and the residual chemical potential μ_i^{res}, are functions of the residual Helmholtz energy (a^{res}), as expressed in eqs 7 and 8.

$$Z = 1 + \rho\left(\frac{\partial(a^{res}/k_B T)}{\partial\rho}\right) \quad (7)$$

dx.doi.org/10.1021/mp400729x | Mol. Pharmaceutics 2014, 11, 2294−2304

$$\frac{\mu_i^{res}}{k_B T} = \frac{a^{res}}{k_B T} + Z - 1 + \left(\frac{\partial(a^{res}/k_B T)}{\partial x_i}\right) - \sum_{j-1}^{N} x_j \left(\frac{\partial(a^{res}/k_B T)}{\partial x_j}\right) \quad (8)$$

Once the activity coefficient of the API γ^{L}_{API} is determined, the API solubility in polymers can be calculated by eq 1.

For the prediction of the LLE, the activity coefficients of both, the API γ^{L}_{API} and polymer $\gamma^{L}_{polymer}$, respectively, have to be used in eqs 2 and 3.

MATERIALS AND METHODS

Materials. Artemisinin was purchased as crystalline powder from Xian BoSheng Biological Technology Co. Ltd. (China) with a purity > 99%. Indomethacin was purchased from Sigma-Aldrich (Germany) with a purity > 99%. Sulfadimidine and sulfathiazole both had a purity > 99% and were purchased from VWR (Germany). PEG 400 was purchased from AppliChem (Germany), PEG 6000 from Prolabo VWR Germany (Germany), and PEG 35000 from Merck VWR (Germany). All substances were used as obtained without any further purification.

Methods. *Sample Preparation for DSC Analysis.* In the case of systems with PEG 6000 and PEG 35000, different physical mixtures of API and PEG with weight fractions of API (w_{API}) of 0.60, 0.75, or 0.90 were prepared. For the sample preparation, the two components were weighed with an accuracy of ±0.3 mg and mortared for at least 5 min until a macroscopically homogeneous powder was obtained. Each sample was prepared in duplicate and measured twice with differential scanning calorimetry (DSC). In the case of the liquid polymer PEG 400, a droplet of polymer was directly introduced into a DSC aluminum pan and weighed with an accuracy of ±0.3 mg. Then, API was added to obtain the preferred weight fraction w_{API}. The samples of API in PEG 400 were prepared and measured in triplicate.

Measurement of API Solubility in PEG. The solubilities of artemisinin and indomethacin as well as sulfathiazole and sulfadimidine in PEG (SLE) were determined with DSC. The DSC apparatus Q 2000 from TA Instruments was calibrated using indium. To maintain an inert atmosphere, the apparatus was purged with nitrogen at a flow rate of 40 mL/min. Ten to 15 mg of an API/PEG solid dispersion of known API weight fraction (w_{API}) was transferred into an aluminum pan and heated from 298.15 K up to 433.15 K for artemisinin, up to 443.15 K for indomethacin, and up to 493.15 K for sulfathiazole and sulfadimidine with a heating rate of 2 K/min.

During the heating process, the API dissolved in the polymer, which was detected through DSC as an endothermic event. The melting temperature of the API/polymer solid dispersion was determined as the temperature at which the dissolution of the API in PEG was completed.[41]

Since this method is dynamic, the obtained temperature depends on the heating rate. To correct for this, the relation between heating rate and measured temperature was investigated for samples with w_{API} of 0.9, which showed the highest endothermic signal to analyze. It was assumed that the obtained relationship is also valid for other weight fractions of the same API. Samples with w_{API} of 0.9 were measured additionally with heating rates of 5 and 10 K/min. It was found that the measured melting temperature decreased linearly with decreasing heating rate, and the melting temperature at equilibrium was obtained by extrapolating to heating rate zero.

The overall average deviation of the measured melting temperatures was estimated to be ±1 K.

RESULTS

Influence of Heating Rate on API Solubility in PEG. The API solubility in polymers was analyzed by DSC measurements. Therefore, the offset of the melting peak was detected as shown by the dashed lines in Figure 4. To determine the influence of the heating rate on the measured melting temperature, samples with API weight fraction w_{API} of 0.9 were measured with heating rates of 2, 5, and 10 K/min.

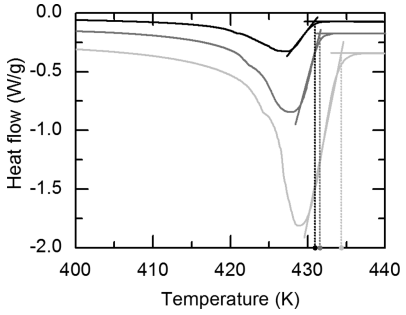

Figure 4. Determination of the melting temperature of solid dispersions of indomethacin in PEG 400 with $w_{indomethacin}$ of 0.9 at different heating rates of 2 K/min (black), 5 K/min (dark gray), and 10 K/min (light gray). The offset of the melting peak was analyzed (dashed lines).

It becomes obvious, that the area of the melting peak increases with increasing heating rate, and therewith, also the measured melting temperature (offset) increases. This influence is visualized by plotting the measured melting temperature versus the heating rate in Figure 5.

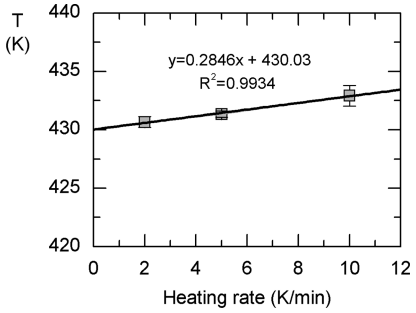

Figure 5. Measured melting temperature of indomethacin in PEG 400 with $w_{indomethacin}$ of 0.9 as a function of heating rate including the equation of the linear correlation.

The results from Figure 5 show that there is a linear correlation between measured melting temperature and applied heating rate. Using the linear correlation given in Figure 5, the melting temperature for a solid dispersion of known composition was extrapolated to a heating rate of zero to obtain the equilibrium value. At this temperature, the API concentration in polymer known by the sample preparation is the solubility of the API in the polymer.

API Solubility in PEG 400, PEG 6000, and PEG 35000. The measured equilibrium temperatures (SLE) at given weight fractions of artemisinin and indomethacin in PEG 400, PEG

Table 1. Measured Equilibrium Temperatures (SLE) at Given Weight Fraction w_{API} of Indomethacin and Artemisinin in PEG 400, PEG 6000, and PEG 35000 and of Sulfathiazole and Sulfadimidine in PEG 35000

		PEG 400	PEG 6000	PEG 35 000
	w_{API} (g/g)	T (K)	T (K)	T (K)
indomethacin	0.9	430.07 ± 1.44	432.21 ± 0.49	432.24 ± 0.62
	0.75	425.75 ± 1.05	427.69 ± 0.58	430.11 ± 0.67
	0.6	418.13 ± 1.15	420.86 ± 0.92	423.54 ± 1.21
artemisinin	0.9	421.59 ± 0.92	423.71 ± 0.85	424.07 ± 0.88
	0.75	417.53 ± 0.88	422.62 ± 0.84	422.79 ± 0.97
	0.6	414.59 ± 0.85	417.69 ± 1.29	419.07 ± 0.84
sulfathiazole	0.9			473.97 ± 0.21
	0.75			470.61 ± 2.38
	0.6			462.06 ± 1.37
	0.45			440.73 ± 0.76
sulfadimidine	0.9			471.85 ± 0.07
	0.75			469.49 ± 0.41
	0.6			463.59 ± 2.07
	0.45			453.93 ± 0.99

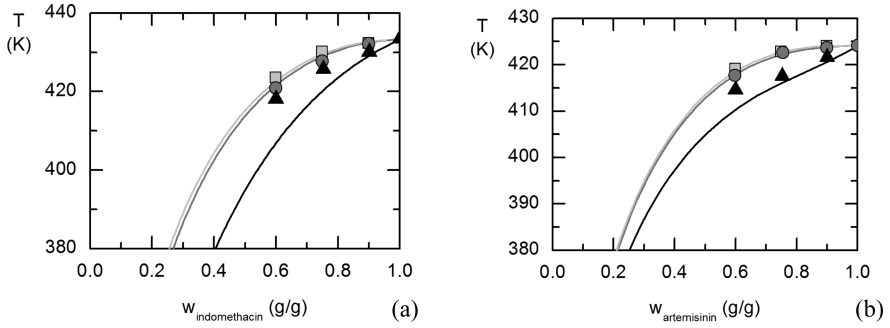

Figure 6. Solubility of indomethacin (a) and artemisinin (b) in PEG as a function of PEG molecular weight. Symbols represent the experimental solubility data of APIs in PEG 400 (triangles), PEG 6000 (circles), and PEG 35000 (squares). The lines show modeling results of PC-SAFT for PEG 400 (black), PEG 6000 (dark gray), and for PEG 35000 (light gray).

6000, and PEG 35000 as well as of sulfathiazole and sulfadimidine in PEG 35000 are listed in Table 1.

Results for indomethacin and artemisinin are also shown in Figure 6. It becomes obvious that the solubility of both, indomethacin and artemisinin, in PEG is a function of molecular weight of PEG and increases in the following order: PEG 35000 < PEG 6000 < PEG 400, whereas the difference between the API solubility in PEG 400 and in PEG 6000 is more significant than the difference between the API solubility in PEG 6000 and PEG 35000. This result is in agreement with results found in literature where the reported solubility of naproxen in PEGs of different molecular weights shows a similar trend.[7] These data were further used to verify the modeling results achieved by PC-SAFT, considering the influence of polymer molecular weight.

Estimation of PC-SAFT Pure-Component Parameters for the APIs. The pure-component PC-SAFT parameters of artemisinin were fitted to experimental solubility data[42] in ethyl acetate, acetone, ethanol, and methanol in the temperature range of 284.15−323.15 K. For indomethacin, the pure-component parameters were fitted to experimental solubility data in ethanol, methanol, acetonitrile, 2-propanol, and toluene in the temperature range of 290.15−312.15 K.[43]

According to its chemical structure, indomethacin was regarded as an associating molecule with six association sites N_i^{assoc} (three electron acceptors and three electron donors) (see Figure 3). The association-volume parameter was set to 0.02. Thus, four parameters, namely, the segment number m_i^{seg}, segment diameter σ_i, dispersion-energy parameter u_i/k_B, and association-energy parameter ε^{AiBj}/k_B had to be fitted for indomethacin. Artemisinin was treated as a molecule with induced association[24] because it only carries groups that can act as proton acceptors but not as proton donors. This means that artemisinin cannot associate as a pure component but can associate in mixtures with molecules that have proton-donor properties. As usually done in those cases, the association-volume parameter of artemisinin was set equal to one of the other components in the mixture and the association-energy parameter was set as zero.[24] This means that three parameters, namely, the segment number m_i^{seg}, segment diameter σ_i, and dispersion-energy parameter u_i/k_B, were fitted for artemisinin. The association sites of artemisinin were set to one proton acceptor and to one proton donator since it was already found earlier; small molecules like solvents or APIs are best modeled using this association scheme.[24]

For the PC-SAFT predictions of the sulfonamides in PEG 35000 and PVP K10, solubility data of sulfamerazine in octanol in a range of 298−313 K[44] and 2-propanol at 298 K[45] were used to fit the pure-component parameters of sulfamerazine. Because of the similar chemical structure of the four considered sulfonamides (see Figure 1), the pure-component parameters (except the dispersion-energy parameter u_i/k_B) of the other three sulfonamides were assumed to be identical to those of sulfamerazine. The dispersion-energy parameter for each of the

dx.doi.org/10.1021/mp400729x | Mol. Pharmaceutics 2014, 11, 2294−2304

Table 2. Pure-Component PC-SAFT Parameters of Artemisinin, Indomethacin, Sulfamerazine, Sulfathiazole, Sulfadimidine, and Sulfadiazine Used within This Work

	M (g/mol)	m_i^{seg}	σ_i (Å)	u_i/k_B (K)	ε^{AiBi}/k_B (K)	κ^{AiBi}	N_i^{assoc}
artemisinin	282.34	6.845	2.959	293.763	0	0.02	1/1
indomethacin	357.79	14.283	3.535	262.791	886.4	0.02	3/3
sulfamerazine	264.3	9.847	3.765	400.923	1498.44	0.02	2/2
sulfathiazole	255.3	9.847	3.765	402.097	1498.44	0.02	2/2
sulfadimidine	278.33	9.847	3.765	419.183	1498.44	0.02	2/2
sulfadiazine	250.28	9.847	3.765	412.495	1498.44	0.02	2/2

Table 3. PC-SAFT Pure-Component Parameters of PEG and PVP K10

	m_i^{seg}/M_i (mol/g)	σ_i (Å)	u_i/k_B (K)	ε^{AiBi}/k_B (K)	κ^{AiBi}	N_i^{assoc}
PEG 400[a]	0.0506	2.899	204.6	1799.8	0.02	2/2
PEG 6000[a]	0.0506	2.899	204.6	1799.8	0.02	2/2
PEG 35000[a]	0.0506	2.899	204.6	1799.8	0.02	2/2
PVP K10[b]	0.0407	2.710	205.6	0	0.02	90/90

[a]Parameters from Stoychev et al.[48] [b]Parameters from Prudic et al.[49]

other three sulfonamides was fitted to one experimental solubility data point at 298.15 K. In the cases of sulfathiazole and sulfadiazine, the solubility in 2-propanol[45] was used for that purpose, and for sulfadimidine, we used the solubility in cyclohexane.[46] The PC-SAFT pure-component parameters for the organic solvents were taken from literature.[18,21,28,47]

The pure-component parameters obtained for indomethacin and artemisinin as well as for the sulfonamides are given in Table 2 and were further used in this work to predict the solubility of these APIs in the considered polymers.

Solubility predictions in API/PEG Solid Dispersions as a Function of PEG Molecular Weight. To predict the solubility of indomethacin and artemisinin in PEG as a function of molecular weight, the activity coefficients γ_{API}^{L} of indomethacin and artemisinin were estimated with PC-SAFT using the pure-component parameters of artemisinin and indomethacin in Table 2. The PC-SAFT parameters for PEG were taken from the literature[48] and are listed in Table 3. Since the segment number m_i^{seg} of polymers linearly increases with polymer molecular weight M_i, we list here the ratio m_i^{seg}/M_i, which is constant for a given polymer.

Binary interaction parameters (see Supporting Information, eq A.16) between APIs and polymers were not applied in this work ($k_{ij} = 0$) meaning that all results for API/polymer systems are pure predictions based on pure-component parameters only.

The melting properties of indomethacin, artemisinin, and the four sulfonamides are required to calculate their solubilities in polymers according to eq 1 and are listed in Table 4.

Table 4. Melting Properties of APIs

	T_{API}^{SL} (K)	Δh_{API}^{SL} (kJ/mol)	$\Delta c_{p,API}^{SL}$ (J/(K mol))
artemisinin	424.2[a]	24.3[a]	57.29[b]
indomethacin	433.3[c]	39.3[c]	116.95[c]
sulfamerazine	510.5[d]	36.7[d]	71.89[b]
sulfathiazole	473.8[d]	28.7[d]	60.57[b]
sulfadimidine	470.6[d]	36.0[d]	76.49[b]
sulfadiazine	535.3[d]	39.9[d]	75.88[b]

[a]From Nti-Gyabaah et al.[42] [b]Calculation of entropy of fusion $\Delta s_{API}^{SL} \approx \Delta c_{p,API}^{SL}$ according to Neau et al.[50] [c]From Paus et al.[51] [d]From Caron et al.[52]

Figure 6 shows a comparison of the experimental data obtained within this work with the PC-SAFT solubility prediction of indomethacin and artemisinin in PEG using the above-mentioned parameters as a function of PEG molecular weight.

As shown in Figure 6a, the predicted solubilities of indomethacin in PEG 6000 and PEG 35000 using PC-SAFT are in very good agreement with the experimental data but slightly overestimated for PEG 400. It needs to be mentioned that the PC-SAFT results are purely predicted without fitting to experimental data in Figure 6.

In the case of artemisinin, as shown in Figure 6b, the predicted results from PC-SAFT are for all polymer molecular weights in very good agreement with the experimental data.

The results in Figure 6 demonstrate moreover that PC-SAFT quantitatively predicts the decrease in solubility of indomethacin and artemisinin in PEG with increasing molecular weight of PEG. PC-SAFT also predicts that the solubility difference between the APIs in PEG 6000 and PEG 35000 is smaller than that between PEG 6000 and PEG 400. The maximum relative deviation (MRD) and the average relative deviation (ARD) between calculated and experimental solubilities of artemisinin and indomethacin in PEG were calculated according to eqs 9 and 10.

$$\mathrm{MRD} = 100 \times \max_{i=1,n_{exp}} \left| \frac{w_{calc,i} - w_{exp,i}}{w_{exp,i}} \right| \tag{9}$$

$$\mathrm{ARD} = 100 \times \frac{1}{n_{exp}} \sum_{i=1}^{n_{exp}} \left| \frac{w_{calc,i} - w_{exp,i}}{w_{exp,i}} \right| \tag{10}$$

where n_{exp} represents the number of data points, $w_{calc,i}$ represents the calculated solubility (weight fraction), and $w_{exp,i}$ represents the experimental solubility of the API in the polymer. The results are listed in Table 5.

It becomes clear that the accuracy of the solubility prediction for both APIs is slightly higher in PEG 6000 and PEG 35000 compared to PEG 400. However, the ARD is smaller than 1.5% and the MRD is below 2.7% for all predicted systems, which indicates a good prediction performance of PC-SAFT. The reason for this seems to be that PC-SAFT explicitly accounts for association since both APIs, indomethacin and artemisinin, and PEG are able to interact via hydrogen bonding sites. These

Table 5. Comparison of the Solubility Predictions from PC-SAFT with Experimental Results[a]

	PC-SAFT	
	MRD (%)	ARD (%)
indomethacin		
PEG 400	2.68	1.41
PEG 6000	0.28	0.17
PEG 35000	0.23	0.15
artemisinin		
PEG 400	1.03	0.55
PEG 6000	0.09	0.06
PEG 35000	0.12	0.05

[a]The accuracy is described by MRD and ARD of the calculated and experimental solubilities of indomethacin and artemisinin (w_{API}) in PEG 400, PEG 6000, and PEG 35000.

interactions might be slightly overestimated in the case of indomethacin solubility in PEG 400.

Solubility Predictions in API/Polymer Solid Dispersions as a Function of Polymer. To investigate the influence of polymer on the phase behavior of API/polymer solid dispersions, the solubility of sulfathiazole and sulfadimidine were measured in PEG 35000 and compared with solubility data in PVP K10 from the literature.[52] The experimental results for sulfathiazole are represented in Figure 7 and compared with the predictions from the PC-SAFT modeling. The pure-component parameters for sulfathiazole are listed in Table 2 and of PEG 35000 and PVP K10 in Table 3.

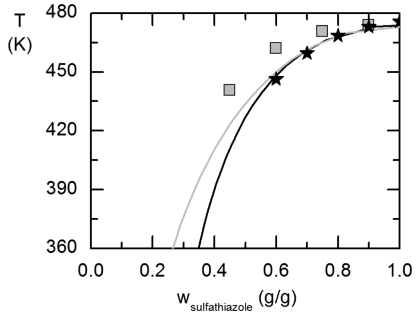

Figure 7. Solubilities of sulfathiazole in PVP K10 (black stars) and PEG 35000 (gray squares). Full lines are predictions of sulfathiazole solubility in PVP K10 (black) and PEG 35000 (gray) using PC-SAFT. Symbols are experimental data, and the data in PVP K10 were taken from the literature.[52]

The results in Figure 7 show that sulfathiazole is experimentally found to be less soluble in PEG than in PVP K10, which is also predicted by PC-SAFT. The higher solubility in PVP might be caused by stronger interactions of sulfathiazole with the amide group of PVP than with the ether and/or hydroxyl group in PEG. The deviation between experimental results and the predictions is higher for the solid dispersions of sulfathiazole in PEG 35000 (ARD: 2.02%) than in PVP K10 (0.24%), but the prediction results are still very reasonable. This trend is similar for PEG and PVP solid dispersions of sulfadimidine listed in Table 6.

The overall ARD is below 3%, which shows a good prediction performance of PC-SAFT as a tool to prescreen an appropriate polymer for a given API.

Solubility Predictions in API/Polymer Solid Dispersions as a Function of API. In addition to the influence of the type of polymer and its molecular weight on the phase behavior of API/polymer solid dispersions, the influence of the API was also investigated in this work. The solubility data of four sulfonamides (sulfamerazine, sulfathiazole, sulfadimidine, and sulfadiazine) in PVP K10 were taken from the literature and used for verification of the results predicted with PC-SAFT (Figure 8).

Table 6. Comparison of Solubility Predictions from PC-SAFT with Experimental Data[a]

	PVP K10		PEG 35000	
	MRD (%)	ARD (%)	MRD (%)	ARD (%)
sulfamerazine	2.37	1.12		
sulfathiazole	0.44	0.24	4.04	2.02
sulfadimidine	5.59	1.76	6.71	2.81
sulfadiazine	4.48	1.68		

[a]The accuracy is described by MRD and ARD of calculated and experimental solubilities for sulfonamides in PVP K10 and PEG 35000.

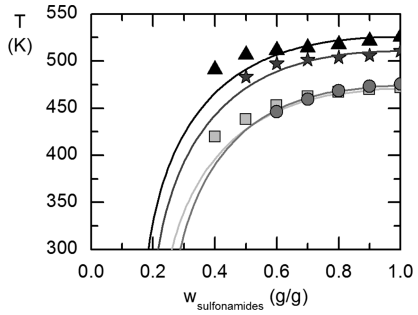

Figure 8. Solubilities of sulfadiazine (black triangles), sulfamerazine (dark gray stars), sulfathiazole (gray circles), and sulfadimidine (light gray squares) in PVP K10. Full lines are predictions of solubilities of sulfadiazine (black), sulfamerazine (dark gray), sulfathiazole (gray), and sulfadimidine (light gray) in PVP using PC-SAFT. Symbols are experimental data taken from the literature.[52]

As shown in Figure 8, the API solubility, of course, also depends on the API type. In this example the solubility in PVP K10 decreases in the following order sulfadiazine > sulfamerazine > sulfadimidine > sulfathiazole. All four examples show that the solubility predictions obtained using PC-SAFT agree qualitatively with the experimental data. The deviation between the modeling results and the experimental data increases with decreasing API content in the solid dispersion (see Table 6).

DISCUSSION

Since more and more high-potential APIs have low solubilities, there is an increasing demand for promising formulations to enhance an API bioavailability. One possibility is the preparation of solid dispersions by integrating the amorphous API into a polymer matrix. A possible amorphous phase separation or the recrystallization of the API is determined by the API/polymer phase diagram (see Figure 2).

In this work it was shown that PC-SAFT is suitable to predict the phase behavior of API/polymer dispersion in the temperature/concentration space as a function of API as well as the type of polymer and polymer's molecular weight.

All obtained experimental results and PC-SAFT predictions are plotted in Figure 9 as the natural logarithm of API solubility

dx.doi.org/10.1021/mp400729x | Mol. Pharmaceutics 2014, 11, 2294−2304

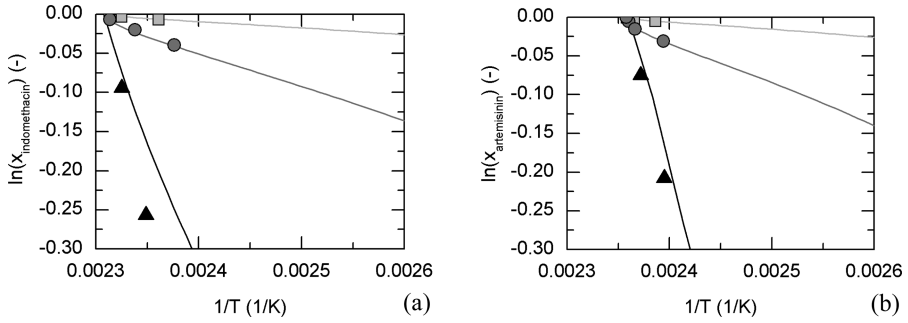

Figure 9. Solubility of indomethacin (a) and artemisinin (b) in PEG as a function of PEG molecular weight. Symbols represent the experimental solubility data of APIs in PEG 400 (triangles), PEG 6000 (circles), and PEG 35000 (squares). The lines show modeling results of PC-SAFT for PEG 400 (black), PEG 6000 (dark gray), and for PEG 35000 (light gray).

(in molar fraction) as a function of $1/T$ to discuss the ideality/nonideality of the solubility behavior.

The results from the plots of $\ln(x)$ over $1/T$ show that the experimental solubilities of indomethacin and artemisinin in PEG as well as the PC-SAFT predictions follow an almost linear trend. This indicates that, assuming a constant heat of fusion in the considered temperature range, the logarithm of the activity coefficient γ^{L}_{API} is either constant or also follows a linear trend over $1/T$ in this temperature/concentration range (see also eq 1).

This does, however, NOT mean that the systems behave thermodynamically ideal since the API activity coefficients do deviate from unity. Figure 10 shows, as an example, the

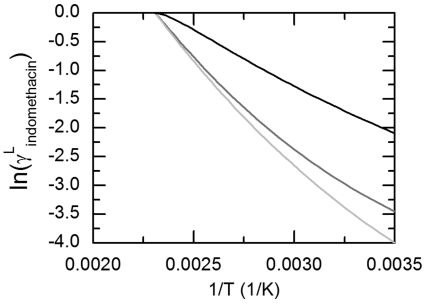

Figure 10. Logarithm of the activity coefficients $\gamma^{L}_{indomethacin}$ of indomethacin in PEG 400 (black), PEG 6000 (dark gray), and PEG 35000 (light gray) over $1/T$ as calculated with PC-SAFT.

numerical values of indomethacin activity coefficients (in particular their logarithms) in PEG 400, PEG 6000, and PEG 35000 and how they change with temperature.

It becomes clear that the logarithms of the indomethacin activity coefficients $\gamma^{L}_{indomethacin}$ in PEG 400, PEG 6000, and PEG 35000 decrease linearly with increasing $1/T$ and therefore increase with increasing temperature. As also to be seen from Figure 10, the indomethacin activity coefficients remarkably deviate from unity (logarithms form zero) at lower temperatures, and these deviations increase with increasing PEG molecular weights. It is therefore worthwhile to use a thermodynamic model like PC-SAFT to estimate and extrapolate the API activity coefficients.

The results in this work show that PC-SAFT is a capable tool to estimate the activity coefficient of API in API/polymer solid dispersions as a function of temperature and further model the API solubility in polymers.

Temperature extrapolation like in Figures 9 and 10 can also be used to safely determine the API solubility in a polymer at room temperature (e.g., for storage applications), which is usually not experimentally accessible. Finally, it should be mentioned that PC-SAFT is also able to predict the absence or presence of an amorphous phase separation (LLE) using the same pure-component parameters as for the solubility calculations. No phase separation was reported in the literature for any of the API/polymer solid dispersions considered within this work. This is again in agreement with the PC-SAFT modeling, which predicted the absence of an LLE for all of these systems.

In summary, it was demonstrated that PC-SAFT is a powerful tool to predict the API solubility in API/polymer dispersions as a function of type of API and polymer as well as of temperature and molecular weight of the polymer. Predictions for binary API/polymer systems were shown to be in at least qualitative agreement and can be, if necessary, improved by fitting a constant binary parameter k_{ij} to a single data point of the solid dispersion.

Although the application of PC-SAFT seems to be more complicated than, e.g., the application of the Flory–Huggins model, its application is obviously advantageous. Every component (API, polymer, water, and organic solvents) is described by pure-component parameters that have a physical meaning and were determined by fitting beforehand to a few easily assessable solubility data in any solvent. All these parameters are just constants and, once determined, can be used for predictions of any phase diagram for any system, at any concentration, any temperature, and any pressure.

■ ASSOCIATED CONTENT

Supporting Information

All the equations within PC-SAFT modeling. Further description of the pure-component parameter fitting of artemisinin and indomethacin as well as of PVP K10. This material is available free of charge via the Internet at http://pubs.acs.org.

■ AUTHOR INFORMATION

Corresponding Author

*(G.S.) Tel: +49-231-755-2635. Fax: +49-231-755-2572. E-mail: g.sadowski@bci.tu-dortmund.de.

Notes

The authors declare no competing financial interest.

■ ACKNOWLEDGMENTS

The authors would like to acknowledge the financial support from CLIB-Graduate Cluster Industrial Biotechnology (AP)

and from the Alexander von Humboldt-Foundation (YJ). All PC-SAFT calculations were performed using the software SolCalc developed at TU Dortmund.

■ ABBREVIATIONS USED

a, Helmholtz energy (J); $\Delta c_{p,\mathrm{API}}^{\mathrm{SL}}$, difference in the solid and the liquid heat capacities of the API (J/(K mol)); $\Delta h_{\mathrm{API}}^{\mathrm{SL}}$, melting enthalpy of pure API (J/mol); k_{B}, Boltzmann constant 1.38065 × 10^{-23} (J/K); k_{ij}, binary interaction parameter; m_{seg}, total number of segments; M, weight-average molar mass (g/mol); $N_{\mathrm{i}}^{\mathrm{assoc}}$, association sites; R, ideal gas constant (J/(K mol)); T, temperature (K); $T_{\mathrm{API}}^{\mathrm{SL}}$, melting temperature of API (K); u/k_{B}, dispersion-energy parameter (K); w, weight fraction; x, mole fraction; Z, compressibility factor; γ, activity coefficient; $\varepsilon^{\mathrm{AiBi}}/k_{\mathrm{B}}$, association-energy parameter (K); φ, fugacity coefficient; κ^{AiBi}, association-energy volume; μ, chemical potential (J/mol); API, active pharmaceutical ingredient; i,j, component indexes; seg, segment; 0, pure substance; A_i, B_i, association sites A and B of molecule i; assoc, association; disp, dispersion; hc, hard chain; hs, hard sphere; L, liquid; S, solid; SL, solid−liquid; ARD, average relative deviation; API, active pharmaceutical ingredient; LLE, liquid−liquid equilibrium; MRD, maximum relative deviation; SLE, solid−liquid equilibrium

■ REFERENCES

(1) Leuner, C.; Dressman, J. Improving drug solubility for oral delivery using solid dispersions. *Eur. J. Pharm. Biopharm.* **2000**, *50*, 47−60.
(2) Vasconcelos, T.; Sarmento, B.; Costa, P. Solid dispersions as strategy to improve oral bioavailability of poor water soluble drugs. *Drug Discovery Today* **2007**, *12*, 1068−1075.
(3) Chiou, W. L.; Riegelmann, S. Pharmaceutical applications of solid dispersion systems. *J. Pharm. Sci.* **1971**, *60*, 1281−1302.
(4) Qian, F.; Huang, J.; Hussain, M. A. Drug−polymer solubility and miscibility: Stability consideration and practical challenges in amorphous solid dispersion development. *J. Pharm. Sci.* **2010**, *99*, 2941−7.
(5) Newman, A.; Knipp, G.; Zografi, G. Assessing the performance of amorphous solid dispersions. *J. Pharm. Sci.* **2012**, *101*, 1355−77.
(6) Ford, J. L.; Stewart, A. F.; Dubois, J.-L. The properties of solid dispersions of indomethacin or phenylbutazone in polyethylene glycol. *Int. J. Pharm.* **1986**, *28*, 11−22.
(7) Mura, P.; Manderioli, A.; Bramanti, G.; Ceccarelli, L. Properties of solid dispersions of naproxen in various polyethylene glycols. *Drug Dev. Ind. Pharm.* **1996**, *22*, 909−916.
(8) Craig, D.; Newton, J. The dissolution of nortriptyline HCl from polyethylene glycol solid dispersions. *Int. J. Pharm.* **1992**, *78*, 175−182.
(9) Corrigan, O. I.; Murphy, C. A.; Timoney, R. P. Dissolution properties of polyethylene glycols and polyethylene glycol−drug systems. *Int. J. Pharm.* **1979**, *4*, 67−74.
(10) Sun, Y.; Tao, J.; Zhang, G. G. Z.; Yu, L. Solubilities of crystalline drugs in polymers: An improved analytical method and comparison of solubilities of indomethacin and nifedipine in PVP, PVP/VA, and PVAc. *J. Pharm. Sci.* **2010**, *99*, 4023−4031.
(11) Marsac, P. J.; Li, T.; Taylor, L. S. Estimation of drug−polymer miscibility and solubility in amorphous solid dispersions using experimentally determined interaction parameters. *Pharm. Res.* **2009**, *26*, 139−51.
(12) Tao, J.; Sun, Y.; Zhang, G. G. Z.; Yu, L. Solubility of small-molecule crystals in polymers: D-mannitol in PVP, indomethacin in PVP/VA, and nifedipine in PVP/VA. *Pharm. Res.* **2009**, *26*, 855−864.
(13) Flory, P. J. Thermodynamics of high polymer solutions. *J. Chem. Phys.* **1942**, *10*, 51−61.
(14) Hansen, C. M. The three-dimensional solubility parameter-key to paint component affinities: solvents, plasticizers, polymers, and resins. II. Dyes, emulsifiers, mutual solubility and compatibility, and pigments. III. Independent calculation of the parameter components. *J. Paint Technol.* **1967**, *39*, 505−510.
(15) Greenhalgh, D. J.; Williams, A. C.; Timmins, P.; York, P. Solubility parameters as predictors of miscibility in solid dispersions. *J. Pharm. Sci.* **1999**, *88*, 1182−90.
(16) Tian, Y.; Booth, J.; Meehan, E.; Jones, D. S.; Li, S.; Andrews, G. P. Construction of drug−polymer thermodynamic phase diagrams using Flory−Huggins interaction theory: identifying the relevance of temperature and drug weight fraction to phase separation within solid dispersions. *Mol. Pharmaceutics* **2013**, *10*, 236−48.
(17) Paudel, A.; van Humbeeck, J.; van den Mooter, G. Theoretical and experimental investigation on the solid solubility and miscibility of naproxen in poly(vinylpyrrolidone). *Mol. Pharmaceutics* **2010**, *7*, 1133−1148.
(18) Gross, J.; Sadowski, G. Perturbed-chain SAFT: An equation of state based on a perturbation theory for chain molecules. *Ind. Eng. Chem. Res.* **2001**, *40*, 1244−1260.
(19) Gross, J.; Spuhl, O.; Tumakaka, F.; Sadowski, G. Modeling copolymer systems using the perturbed-chain SAFT equation of state. *Ind. Eng. Chem. Res.* **2003**, *42*, 1266−1274.
(20) Schäfer, E.; Sadowski, G. Liquid−liquid equilibria of systems with linear aldehydes. Experimental data and modeling with PCP-SAFT. *Ind. Eng. Chem. Res.* **2012**, *51*, 14525−14534.
(21) Gross, J.; Sadowski, G. Application of the perturbed-chain SAFT equation of state to associating systems. *Ind. Eng. Chem. Res.* **2002**, *41*, 5510−5515.
(22) Ghosh, A.; Chapman, W. G.; French, R. N. Gas solubility in hydrocarbons: A SAFT-based approach. *Fluid Phase Equilib.* **2003**, *209*, 229−243.
(23) Aparicio, S. Phase equilibria in perfluoroalkane + alkane binary systems from PC-SAFT equation of state. *J. Supercrit. Fluids* **2008**, *46*, 10−20.
(24) Kleiner, M.; Sadowski, G. Modeling of polar systems using PCP-SAFT: An approach to account for induced-association interactions. *J. Phys. Chem. C* **2007**, *111*, 15544−15553.
(25) Tihic, A.; Kontogeorgis, G. M.; von Solms, N.; Michelsen, M. L.; Constantinou, L. A predictive group-contribution simplified PC-SAFT equation of state: Application to polymer systems. *Ind. Eng. Chem. Res.* **2007**, *47*, 5092−5101.
(26) Gross, J.; Sadowski, G. Modeling polymer systems using the perturbed-chain statistical associating fluid theory equation of state. *Ind. Eng. Chem. Res.* **2002**, *41*, 1084−1093.
(27) Prikhod'ko, I. V.; Tumakaka, F.; Sadowski, G. Application of the PC-SAFT equation of state to modeling of solid-liquid equilibria in systems with organic components forming chemical compounds. *Russ J. Appl. Chem.* **2007**, *80*, 542−548.
(28) Ruether, F.; Sadowski, G. Modeling the solubility of pharmaceuticals in pure solvents and solvent mixtures for drug process design. *J. Pharm. Sci.* **2009**, *98*, 4205−15.
(29) Paduszyński, K.; Domańska, U. Thermodynamic modeling of ionic liquid systems: development and detailed overview of novel methodology based on the PC-SAFT. *J. Phys. Chem. B* **2012**, *116*, 5002−5018.
(30) Kouskoumvekaki, I. A.; von Solms, N.; Lindvig, T.; Michelsen, M. L.; Kontogeorgis, G. M. Novel method for estimating pure-component parameters for polymers: Application to the PC-SAFT equation of state. *Ind. Eng. Chem. Res.* **2004**, *43*, 2830−2838.
(31) Ferrando, N.; de Hemptinne, J.-C.; Mougin, P.; Passarello, J.-P. Prediction of the PC-SAFT associating parameters by molecular simulation. *J. Phys. Chem. B* **2011**, *116*, 367−377.
(32) Cassens, J.; Prudic, A.; Ruether, F.; Sadowski, G. Solubility of pharmaceuticals and their salts as a function of pH. *Ind. Eng. Chem. Res.* **2013**, *52*, 2721−2731.
(33) Kiesow, K.; Tumakaka, F.; Sadowski, G. Experimental investigation and prediction of oiling out during crystallization process. *J. Cryst. Growth* **2008**, *310*, 4163−4168.
(34) Marsac, P. J.; Konno, H.; Rumondor, A. C.; Taylor, L. S. Recrystallization of nifedipine and felodipine from amorphous

molecular level solid dispersions containing poly(vinylpyrrolidone) and sorbed water. *Pharm. Res.* **2008**, *25*, 647−56.
(35) Karavas, E.; Ktistis, G.; Xenakis, A.; Georgarakis, E. Miscibility behavior and formation mechanism of stabilized felodipine-polyvinylpyrrolidone amorphous solid dispersions. *Drug Dev. Ind. Pharm.* **2005**, *31*, 473−489.
(36) Vasanthavada, M.; Tong, W. Q.; Joshi, Y.; Kislalioglu, M. S. Phase behavior of amorphous molecular dispersions I: Determination of the degree and mechanism of solid solubility. *Pharm. Res.* **2004**, *21*, 1598−1606.
(37) Hancock, B. C.; Shamblin, S. L.; Zografi, G. Molecular mobility of amorphous pharmaceutical solids below their glass transition temperatures. *Pharm. Res.* **1995**, *12*, 799−806.
(38) Gordon, M.; Taylor, J. S. Ideal copolymers and the second-order transitions of synthetic rubbers. I. Non-crystalline copolymers. *J. Appl. Chem.* **1952**, *2*, 493−500.
(39) Kelley, F. N.; Bueche, F. Viscosity and glass temperature relations for polymer-diluent systems. *J. Polym. Sci.* **1961**, *1*, 549−556.
(40) Prausnitz, J. M.; Lichtenthaler, R. N.; De Azevedo, E. G. *Molecular Theory of Fluid-Phase Equilibria*, 3rd.; Prentice Hall: Upper Saddle River, NJ, 1999.
(41) Mohan, R.; Lorenz, H.; Myerson, A. S. Solubility measurement using differential scanning calorimetry. *Ind. Eng. Chem. Res.* **2002**, *41*, 4854−4862.
(42) Nti-Gyabaah, J.; Gbewonyo, K.; Chiew, Y. C. Solubility of Artemisinin in Different Single and Binary Solvent Mixtures Between (284.15 and 323.15) K and NRTL Interaction Parameters. *J. Chem. Eng. Data* **2010**, *55*, 3356−3363.
(43) Measured by Prudic, A., TU Dortmund, 2013.
(44) Martínez, F.; Gómez, A. Thermodynamic study of the solubility of some sulfonamides in octanol, water, and the mutually saturated solvents. *J. Solution Chem.* **2001**, *30*, 909−923.
(45) Regosz, A.; Pelplinska, T.; Kowalski, P.; Thiel, Z. Prediction of solubility of sulfonamides in water and organic solvents based on the extended regular solution theory. *Int. J. Pharm.* **1992**, *88*, 437−442.
(46) Martínez, F.; Ávila, C. M.; Gómez, A. Thermodynamic study of the solubility of some sulfonamides in cyclohexane. *J. Braz. Chem. Soc.* **2003**, *14*, 803−808.
(47) Kleiner, M.; Gross, J. An equation of state contribution for polar components: Polarizable dipoles. *AIChE J.* **2006**, *52*, 1951−1961.
(48) Stoychev, I.; Galy, J.; Fournel, B.; Lacroix-Desmazes, P.; Kleiner, M.; Sadowski, G. Modeling the phase behavior of PEO-PPO-PEO surfactants in carbon dioxide using the PC-SAFT equation of state: Application to dry decontamination of solid substrates. *J. Chem. Eng. Data* **2009**, *54*, 1551−1559.
(49) Prudic, A.; Ji, Y. H.; Sadowski, G. Phase behavior of solid dispersions as function of relative humidity. Manuscript in preparation.
(50) Neau, S. H.; Bhandarkar, S. V.; Hellmuth, E. W. Differential molar heat capacities to test ideal solubility estimations. *Pharm. Res.* **1997**, *14*, 601−605.
(51) Paus, R., Ji, Y. H.; Sadowski, G. Dissolution of crystalline active pharmaceutical ingredients: Experimental investigation and modeling by a thermodynamic approach. Manuscript in preparation.
(52) Caron, V.; Hu, Y.; Tajber, L.; Erxleben, A.; Corrigan, O. I.; McArdle, P.; Healy, A. M. Amorphous solid dispersions of sulfonamide/soluplus® and sulfonamide/PVP prepared by ball milling. *AAPS PharmSciTech* **2013**, *14*, 464−474.